Building and Environment 188 (2021) 107509

Contents lists available at ScienceDirect

Building and Environment

journal homepage: http://www.elsevier.com/locate/buildenv

Simplified direct forcing approach for dynamic modeling of building natural ventilation

Wentao Wu [a], Jung Min Han [b,*], Ali Malkawi [b]

[a] Department of Civil and Architectural Engineering, College of Engineering, Tennessee State University, Nashville, 37209, TN, USA
[b] Harvard Center for Green Buildings and Cities, Graduate School of Design, Harvard University, Cambridge, 02138, MA, USA

ARTICLE INFO

Keywords:
Passive cooling
Energy efficiency
Windows
CFD
Demand-controlled ventilation

ABSTRACT

Natural ventilation is a promising approach to provide passive cooling in highly energy efficient buildings. A widely applied method to evaluate the performance of natural ventilation is computational fluid dynamics (CFD). However, dynamic modeling of natural ventilation from 1 h to the next is very challenging because state-of-the-art CFD simulations treat windows as fixed wall boundary surfaces. The objective of this study is to propose a direct forcing approach to implement dynamic window operations in CFD simulations. The direct forcing approach marks a band of computational cells according to window positions, and adds an ad-hoc body force to the momentum equations and turbulence production term to the kinetic energy equation. The direct forcing approach shows a high level of performance when predicting volume flow rates through window apertures. The relative deviation was found to vary between 2.2% and 14%, depending on the reference wind speeds. Direct forcing also showed good performance when predicting the height of the neutral plane when the wind incident angle was less than 135°. The direct forcing approach can be applied to study the dynamic daily or weekly CO_2 variations in naturally ventilated buildings with predefined control algorithms. Future work will consider the influence of wall shear stresses and zero normal velocity to improve the accuracy of the direct forcing approach as applied to wind incident angles larger than 135°.

1. Introduction

Global warming is evidenced by the relentless rise in the level of atmospheric carbon dioxide (CO_2), which since the 1950s has increased from 300 ppm to 420 ppm. The US is currently responsible for 21% of the global CO_2 emissions, of which 98% originates from energy consumption [1]. Residential and commercial buildings account for 41% of the energy use in the US [2], and are significant components that exacerbate climate change. In response to this enormous building energy consumption, federal and state governments have promulgated regulatory mandates to achieve zero-energy building targets by 2050 [3]. An ongoing challenge with zero-energy buildings is how to reduce the energy use for space cooling, heating, and ventilation, which accounts for 60%–70% of the total energy consumption [4]. Earlier studies have shown that natural ventilation is a promising approach to provide passive cooling and satisfy the requirements of fresh air and thermal comfort [5]. Natural ventilation is driven by wind pressure and buoyancy forces, without the electricity consumption or limited energy use required for motors to operate windows, and as such it is a sustainable method for improving building energy efficiency.

Natural ventilation through single-sided openings in buildings is an energy-efficient method for adjusting indoor thermal comfort. One challenge with single-sided natural ventilation is determining the ventilation rate. Gough et al. [6] conducted a full-scale experiment to test the single-sided ventilation rates of small window openings in a sheltered building in a limited staggered array in order to simulate turbulent flows in dense urban areas. The result showed that including wind direction and turbulence intensity could improve the accuracy of ventilation rate predictions. Gough et al. [7] compared tracer gas and pressure-based methods for measuring single-sided natural ventilation, and concluded that there was no discernible linear relationship between the ventilation rates obtained from the two methods. Liu et al. [8] applied computational fluid dynamics (CFD) to study the effects of entrance type on natural ventilation in a subway station. The authors revealed that the pressure coefficients used to determine ventilation rates were affected by both outdoor and indoor airflows. Arinami et al. [9] performed large-eddy simulations (LES) to evaluate the effects of guide vanes and adjacent obstacles on the effectiveness of single-sided

* Corresponding author.
E-mail addresses: jhan2@gsd.harvard.edu, jhan2harvard@gmail.com (J.M. Han).

https://doi.org/10.1016/j.buildenv.2020.107509
Received 15 June 2020; Received in revised form 11 November 2020; Accepted 2 December 2020
Available online 7 December 2020

natural ventilation. They incorporated the concept of fresh air arrival rate to quantify the contribution of fluctuating velocities to the ventilation rate. Pan et al. [10] developed a simple model for calculating ventilation rate for an apartment with single-sided natural ventilation that considered both buoyancy and pressure effects. The model showed an average error of 13.1% and a better performance than existing models in literature. Larsen et al. [11] compared the EN16798–7:2017 new equation and EN15242:2007 old equation for single-sided natural ventilation to wind tunnel measurements, full-scale measurements, and CONTAM calculations in order to clarify whether the new equation was more accurate. The authors concluded that the new equation predicted the average airflow rate in a more conservative way. King et al. [12] developed time-dependent CFD models to study the single-sided natural ventilation of a cubic building under eight wind directions. Their results showed that vortex shedding from upwind buildings provided pulsating ventilation. Marzban et al. [13] developed an evolutionary approach based on a genetic algorithm for designing façades with single-sided natural ventilation. The model enabled mapping of the façade design options and evolution of the performance targets. Wang et al. [14] used CFD simulations to test typical windows in order to evaluate their buoyancy-driven single-sided ventilation performance. The results showed that buildings' thermal flow profiles varied by window type even with the same opening areas, and provided relevant analytical equations for calculating flow estimations. Their work also indicated that it was not suitable to use fixed constant discharge coefficients to estimate ventilation rates for real-world window configurations. Zhou et al. [15] developed a model for predicting the total flow rate for single-sided natural ventilation. The new model showed that pulsating flow determined the total flow rate when the window opening area was small, and mean flow determined the total flow rate in the case of larger window opening areas.

The complexity of control strategies for operating windows often prevents the broad application of natural ventilation. Applying heuristic control algorithms to natural ventilation systems may lead to zero-hours of ventilation in the summer in hot-summer climate zones [16]. Conversely, model predictive control is able to trigger natural ventilation at different hours of the day, resulting in cooling energy savings of up to 13% [16]. Compared to mechanical ventilation, the implementation of control strategies for natural ventilation requires further study regarding outdoor environmental factors including wind speed, wind direction, outdoor air temperature, and outdoor air quality. This is due to the inherent nature of natural ventilation: its coupling of the outdoor and indoor environments [17]. For example, outdoor air pollutants can reduce the use of natural ventilation by 5%–70%, depending on the level of pollution [18].

Various control strategies have been proposed for natural ventilation, including spontaneous occupant control, informed occupant control, heuristic automatic control, model predictive control [16], and demand control based on the indoor CO_2 level [19]. These control strategies are rarely tested and implemented in full-scale buildings [20]. This may be due to an inadequate number of buildings designed with natural ventilation and sophisticated software platforms for testing control algorithms. Another likely reason is that very few efficient methods exist for checking whether a natural ventilation system can provide sufficient fresh air. It is challenging to monitor and predict air exchange rates for different opening angles [21]. Natural ventilation rates are affected by dynamic weather conditions, urban morphology [22], building layout and orientation, and especially the size, position, and shape of window apertures [23]. The methods available for determining natural ventilation rates are tracer gas decay, constant tracer gas, and pressure difference [24]. Tracer gas decay method is used to determine indoor ventilation rates under static wind conditions [25], and is not appropriate for dynamic monitoring to provide data for natural ventilation control. Constant tracer gas can be used to estimate dynamic natural ventilation rates with varying external wind conditions; it has been applied to livestock buildings, with respired CO_2 serving as a natural tracer gas [26]. However, it is not feasible for residential and commercial buildings, as it will interfere with daily operations due to public health and safety considerations. The pressure difference method can predict volume flow rates through window apertures, but its agreement with the tracer gas method is often poor [27]. The pressure difference method requires knowledge of the discharge coefficient as it changes with the external wind direction, making it difficult to use in determining dynamic natural ventilation rates [27]. Therefore, in the existing literature, these control strategies have generally been tested and implemented in modeling tools [28] such as EnergyPlus [29]. Airflow network models [30] have been built in EnergyPlus to calculate dynamic ventilation rates through window openings that are simplified with the effective opening area method [31]. However, the type of window has been found to have a significant impact on the quantification of airflow rate through the window opening [32].

In order to consider window configurations in detail, CFD can be applied to calculate the natural ventilation rate [33]. The majority of state-of-the-art CFD models are essentially static simulations of natural ventilation that focus on the influence of wind conditions [34], opening positions [35], opening shapes [36], the configuration of windows [37], etc. [38]. Transient CFD with LES has been applied to natural ventilation problems since the 1990s [39]. The existing LES are adopted to address the influence of turbulence [40] on volume flow rates through window apertures. These transient simulations essentially provide static ventilation rates for specified building dimensions [41] and window configurations [42] under specific wind conditions. Few CFD simulations have investigated dynamic ventilation rates under varying wind conditions and window opening angles. One constraint on dynamic CFD simulations of natural ventilation is the extremely long computational time compared to airflow network models. It has been shown that weekly simulations can offer insights into the dynamic functions of natural ventilation control strategies [31]. Weekly simulations with CFD are feasible, considering the current computational power and resources available. CFD has already been applied to predict indoor CO_2 concentrations for several hours in one multi-story apartment with natural ventilation [43]. However, window type and opening angle were not considered.

Window type and opening angle are essential components when using CFD as a modeling framework to test natural ventilation control strategies. Current technology for the dynamic modeling of automatic window operations requires the concept of moving mesh [44]. The window surface is defined as a moving object. The mesh is locally adapted and refined near the surface when the window is operated at a new angle. The moving mesh method takes a lengthy amount of time and can easily lead to stability issues for complex geometries. Pre-establishing multiple window surfaces is also a recently proposed method that can be implemented at several pre-defined opening angles [45]. When the window is operated from one discrete angle to another, the nodes representing the wall surface at the previous angle are altered to internal nodes. The internal nodes representing the current angle are changed to wall boundary nodes. The pre-defined surfaces form small angles between one another, and the mesh cells are generally skewed in such regions. Therefore, a new approach representing automatic window operations is needed for dynamic modeling of natural ventilation.

Based on the above literature review, several research gaps regarding natural ventilation have been identified. 1) It is difficult to determine natural ventilation rates. 2) CFD is an appropriate tool for estimating natural ventilation rates; however, effective approaches do not exist for simulating the dynamic operation of windows to predict dynamic ventilation rates under different time-dependent weather conditions. The objective of this study is to develop a mathematical model representing dynamic window operations in CFD simulations. The performance of the new window model has been validated against the conventional method, which treats window surfaces as wall boundaries. A dynamic CFD modeling framework has been established based on the

new dynamic window model and used as a testbed for natural ventilation control algorithms. Demand ventilation control based on indoor CO_2 level has been implemented in the dynamic modeling framework and used to demonstrate the ability of the framework to dynamically model building natural ventilation.

2. Materials and methods

2.1. A simplified direct forcing approach for dynamic window operation in CFD

In conventional CFD simulations, windows providing natural ventilation are modeled as wall boundary surfaces (see Fig. 1a). The window-wall surface is immersed in the air domain. The grid has to conform to the boundary. The challenges in applying the wall boundary method to the dynamic modeling of natural ventilation are as follows:

1) Changes in the window's opening angle require using moving mesh.
2) When the window is open at a small angle (<10°), the conformed cells near the window surface are highly skewed, even for unstructured tetrahedral mesh.

Due to the aforementioned challenges, a simplified direct forcing approach is proposed as a means of mimicking the effect of wall boundary conditions at the physical surface of the window. The direct forcing approach marks a band of cells (see Fig. 1b), according to the window's opening angle and adds an ad-hoc body force to the momentum equations. It was assumed that the body force could be represented by the following direct pressure force:

$$-\frac{1}{\rho\zeta}U_i|U_i| \tag{1}$$

where U_i is the mean air velocity component in the x_i direction [m s^{-1}], x_i is the Cartesian coordinate [m], ρ is the density of air [kg m^{-3}], and ζ is the length scale [m]. The turbulence production of the window-wall surface is modeled as:

$$\frac{1}{\zeta}\left(|U_1|^3 + |U_2|^3\right) \tag{2}$$

where U_1 and U_2 are the mean wind velocity components in the horizontal direction. The merit of the direct forcing approach is that a simple structured mesh (see Fig. 1b) can be generated to improve computational efficiency.

2.2. Test cases

The simplified direct forcing approach was tested in a cubical building (see Fig. 2) with single-sided natural ventilation. The dimensions of the building were 3.6 m × 2.4 m × 3.3 m and it had a window opening of 1 m × 1 m. The window was open at an angle of 30°. The CFD simulations were performed using Ansys Fluent [46]. The computational domain was chosen following the AIJ guidelines [47], and had dimensions of 66 m × 66 m × 16.5 m. The enlarged horizontal dimensions allowed for the simulation of scenarios with different wind incident angles. The total cell number was 1.4 million; the smallest cell distance was 0.25 m, based on a mesh convergence study. The speed of the approaching wind was assumed to obey a power law profile with an exponent of 0.14. The reference wind speed and direction varied in different test cases (see Table 1). Choices among the four reference wind speeds were made to ensure the validity of the direct forcing approach within a large span of external wind conditions. The reference height for the reference wind velocities was 8.5 m. The turbulence fluctuation at the inlet boundary was approximated using a widely validated method [48]. The inlet and outlet were determined by the wind's incident angle. For example, when the wind approached at 45°, the two lateral and upwind surfaces were specified as inlets and the two lateral and downwind surfaces were defined as outlets. A fixed pressure was imposed at the outlet. A symmetrical boundary condition was imposed at the top of the domain. The other surfaces were defined as wall boundary surfaces. Wall functions were applied to solve the airflow near the wall surfaces. The scalable wall function applied in this study blended a standard wall function and low Reynolds number formulation, based on a critical y+ value of 11. The Reynolds-averaged Navier-Stokes (RANS) equations with the realizable k-ε model [49] were adopted to solve the turbulent flow. The advection terms in the governing equations

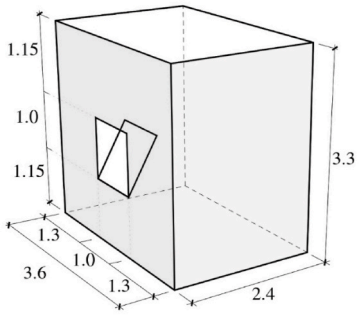

Fig. 2. Building geometry.

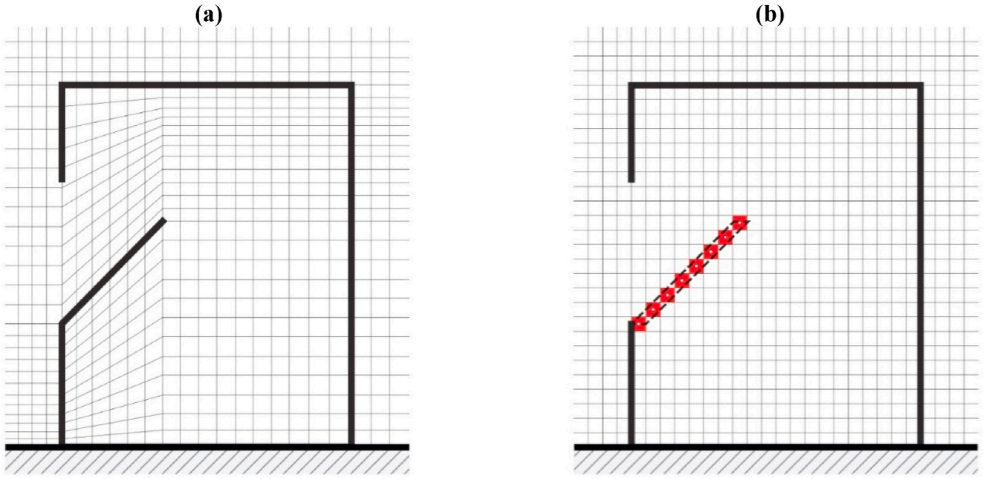

Fig. 1. Cross-section view: (a) the wall boundary and (b) simplified direct forcing approaches to represent window operation in CFD.

Table 1
Simulation cases, boundary conditions, and window representation approach.

Case	Wind incident angle	Wind speed	Approach
1_1	0	3.5	Wall boundary
1_2	0	5.4	Wall boundary
1_3	0	9	Wall boundary
1_4	0	12	Wall boundary
1_5	45	3.5	Wall boundary
1_6	90	3.5	Wall boundary
1_7	135	3.5	Wall boundary
1_8	180	3.5	Wall boundary
2_1	0	3.5	Direct forcing
2_2	0	5.4	Direct forcing
2_3	0	9	Direct forcing
2_4	0	12	Direct forcing
2_5	45	3.5	Direct forcing
2_6	90	3.5	Direct forcing
2_7	135	3.5	Direct forcing
2_8	180	3.5	Direct forcing

Zero-incident wind angle or direction is defined as perpendicular to the window opening.

were discretized by a second-order upwind scheme. The SIMPLE algorithm was adopted for velocity-pressure coupling.

2.3. Dynamic simulations

The motivation for developing this direct forcing approach was to facilitate dynamic simulations of natural ventilation with dynamic windows operations. Thus, dynamic simulations were applied to the same cubical building (see Fig. 2). The transient RANS equations were solved at a timestep of 1 second. The time term was discretized by a first-order implicit scheme. The other numerical schemes were the same as in the test cases. Time-dependent external wind profiles were applied at the inlet. The profiles followed the power law with an exponent of 0.14. The reference wind speeds were sampled every 5 minutes from a local weather station on the roof of the building (11 m above ground) and normalized by the maximum wind speed (3.3 m s^{-1}) during the 10 sample hours. The normalized reference wind speed is shown in Fig. 8. The wind direction was almost constant during the 10 sample hours. The symmetrical boundary condition was imposed at the top and lateral sides of the domain. Fixed pressure was applied to the outlet boundary. The other surfaces were defined as wall boundary surfaces. A single occupant was assumed to generate 500 L of CO_2 per day. The generation of CO_2 was added to a cubical volume of 0.1 m^3 that was 1 m above ground. The cubical volume mimicked the CO_2 stream from the mouth of a sitting person. Heat transfer was not included in this study because the major objective of the research was to test the performance of the direct forcing approach when representing dynamic window operations. The window was operated according to the indoor CO_2 level to mimic the demand ventilation control. Variations in the CO_2 concentration were implemented by a pre-defined occupancy schedule (see Fig. 3). The choice of occupancy schedule was not based on a practical situation. Instead, the schedule ensured time-dependent CO_2 variations in the room. Hence, the windows could be operated more frequently to test the performance of the direct forcing approach. The rule for the CO_2-based demand ventilation control is shown in Table 2; the outdoor CO_2 concentration was assumed to be constant (400 ppm). In total, 10 hours of one day were simulated to demonstrate the dynamic indoor environment resulting from the CO_2-based demand control.

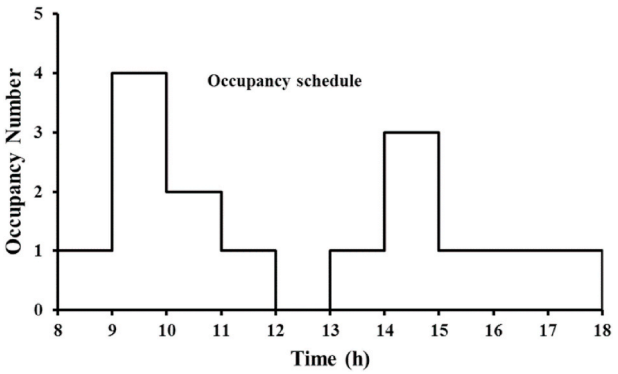

Fig. 3. Pre-defined occupancy schedule.

2.4. Parameters for evaluating the performance of the direct forcing approach

The first parameter for evaluating the performance of the direct forcing approach was the mean volume flow rate (Q_w) through the window aperture:

$$Q_w = \frac{1}{2}\left|U_{w,i}\right|\Delta A_{w,i} \tag{3}$$

where $U_{w,i}$ is the ith velocity component through the window opening and $\Delta A_{w,i}$ is the ith area component of the associated cell. The Einstein summation rule applies to Equation (3). The second parameter used to evaluate the performance of the direct forcing approach was the height of the neutral plane at the window opening aperture. The neutral plane is the position where the outdoor and indoor static pressures are equal. Quantification of the height of the neutral plane is a crucial input for other models such as semi-empirical approach [32].

2.5. Validation of the realizable k-ε model for single-sided natural ventilation

The wind tunnel experiment for single-sided natural ventilation [39] was adopted in this study to verify and validate the CFD analyses. The dimensions of the building model for the wind tunnel experiment are shown in Fig. 4. The horizontal air velocities measured along the three vertical lines (i.e., the red dashed lines) were compared with the data extracted from the CFD simulation, based on the realizable k-ε turbulence model. The horizontal velocities from both the experiment and CFD were normalized by the reference velocity at the inlet and are shown in Fig. 4. The solid lines in the velocity profiles represent the CFD simulation results obtained in this study. The circles indicate the experimental results. Very good agreement inside the building space (below 0.25 m) was observed between the experiment and simulation.

3. Results

3.1. Volume flow rates through the window aperture

The volume flow rates through the window aperture for the two approaches are compared in Fig. 5, including the conventional CFD method that treats the window surface as a wall boundary and the simplified direct forcing approach. The direct forcing approach was able to predict the volume flow rate when the approaching wind was perpendicular to the window aperture (see Fig. 5a). The maximum relative deviation was 14%, which occurred at a low reference wind

Table 2
Window opening angle versus indoor CO_2 level.

Indoor CO_2 concentration (ppm)	Window opening angle (°)
≤500	0
500–700	10
700–900	20
900-1100	30
1100–1300	40
>1300	50

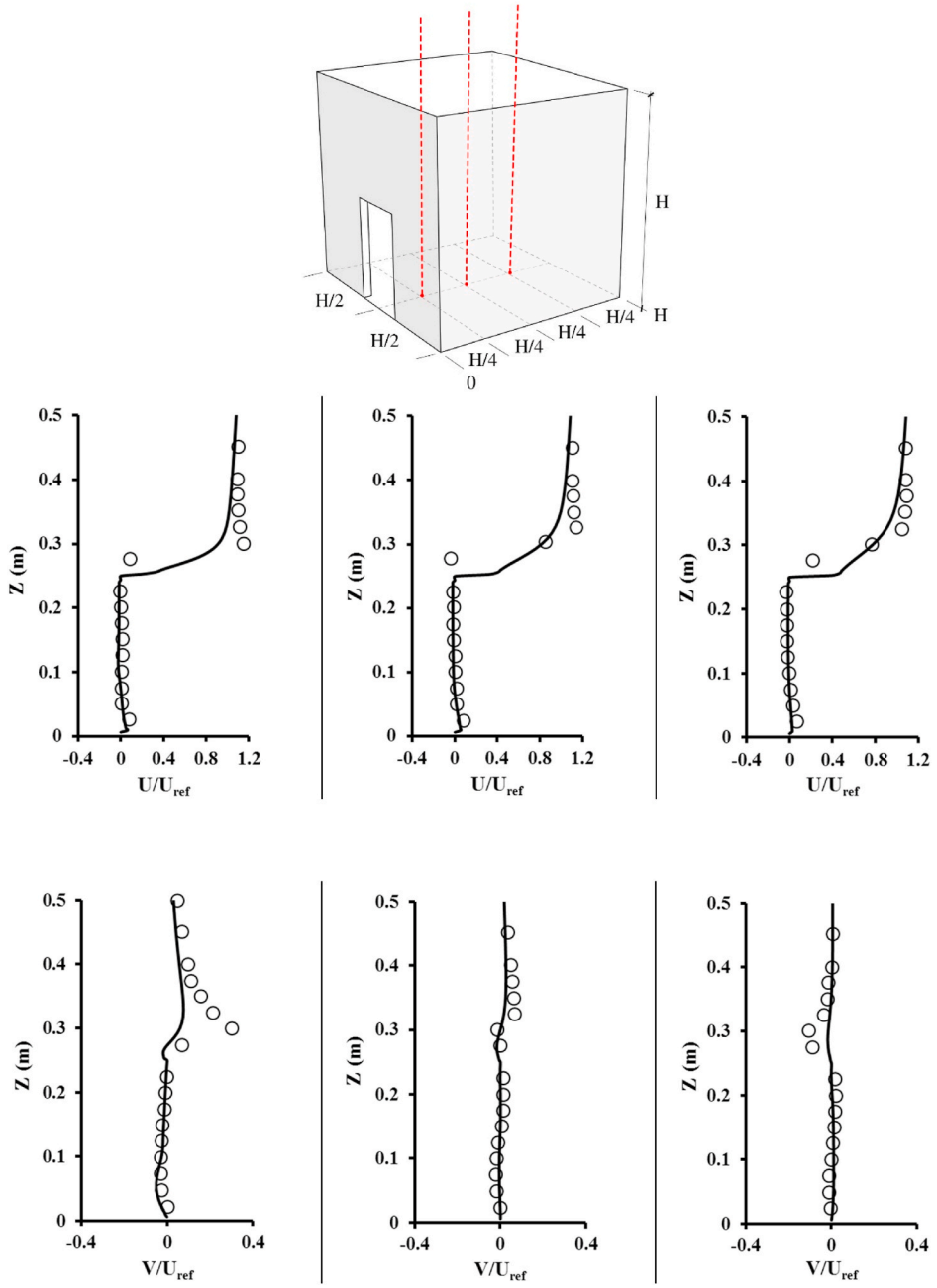

Fig. 4. Validation of the single-sided natural ventilation with wind tunnel data [39]. Circles: wind tunnel data; Solid lines: CFD data. *H* is the height of the building geometry for validation, *Z* is the coordinate in the vertical direction, *U* and *V* are horizontal velocities, and U_{ref} is the reference velocity at the inlet.

speed of 3.5 m s^{-1}. When the wind speed increased, the relative deviation decreased to a value below 2.2%. With the increase in wind speed from 3.5 to 12 m s^{-1}, the volume flow rate increased from 0.042 m^3 s^{-1} to 0.186 m^3 s^{-1}, as predicted by the direct forcing approach. The direct forcing approach also showed a very good ability to predict the volume flow rate between incident angles of 0° and 135°. The largest relative deviation was 14%. For the wall boundary method, the volume flow rate decreased from 0.049 m^3 s^{-1} to 0.044 m^3 s^{-1} when the incident angle changed from 0° to 45°. However, the direct forcing approach showed an increase in the volume flow rate from 0.042 m^3 s^{-1} to 0.048 m^3 s^{-1}. A large deviation of 50% at 180° was found between the two approaches.

3.2. Height of the neutral plane

The vertical profiles of the velocity component perpendicular to the window aperture were similar at different positions in the aperture when the approaching flow was perpendicular to the window aperture. The profile at the center of the aperture is shown in Fig. 6. Very good agreement was found between the profiles predicted by the two approaches. The difference in the velocity component became larger when the wind speed increased. The neutral plane is the location where the perpendicular velocity is zero. Hence, the height of the neutral plane was 1.60 m irrespective of the external wind speeds, and the neutral level was at about 45% of the window height from the window bottom. The heights of the neutral planes for different wind incident angles are shown in Fig. 7. At the 0° incident angle, the height of the neutral plane was horizontally independent, 1.60 m and 1.56 m for the wall boundary method and direct forcing approach, respectively. The relative difference was only 2.5%. At the 45° incident angle, the height of the neutral plane increased from 1.17 m at the upwind side (negative Y) to 1.81 m at

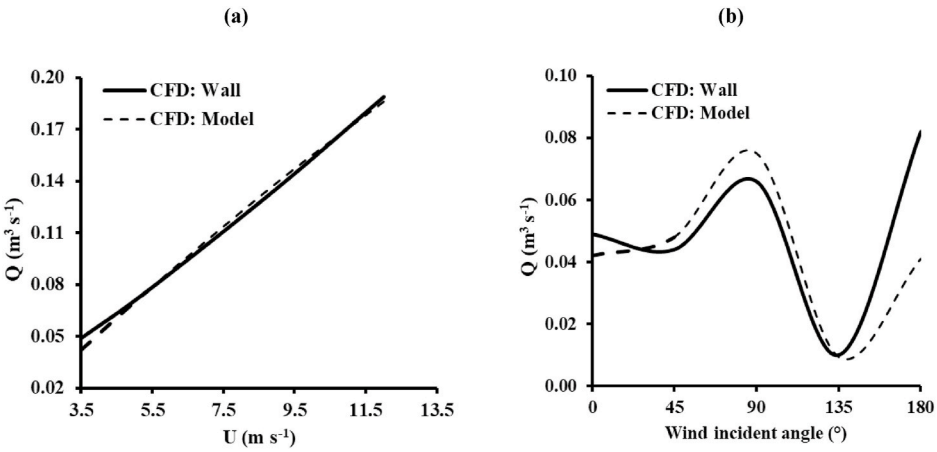

Fig. 5. Comparison of volume flow rates through the window aperture between the wall boundary (Wall) and direct forcing (Model) approaches under different: (a) wind speeds and (b) wind incident angles.

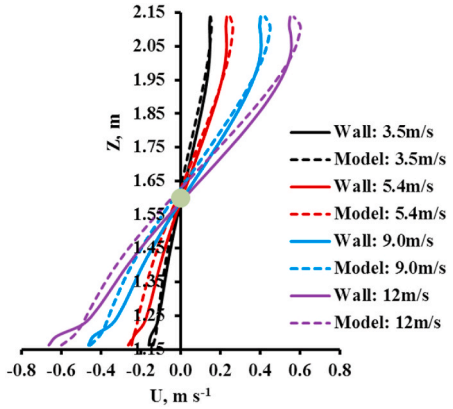

Fig. 6. Heights of the neutral plane under different wind speeds. The wind incident angle was 0°. Wall: wall boundary method; Model: simplified direct forcing approach.

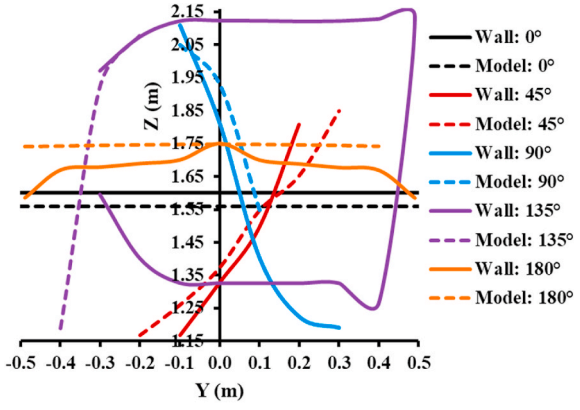

Fig. 7. Heights of the neutral plane under different wind incident angles. The wind speed was 3.5 m s^{-1}. Wall: wall boundary method; Model: simplified direct forcing approach.

the downwind side (positive Y) for the wall boundary method. The maximum relative difference between the two methods was 8.5%. A noticeable difference was the starting and ending horizontal locations of the neutral plane height. The starting locations were at −0.1 m and −0.2 m for the wall boundary and direct forcing approaches, respectively. The ending locations were at 0.2 m and 0.3 m for the wall

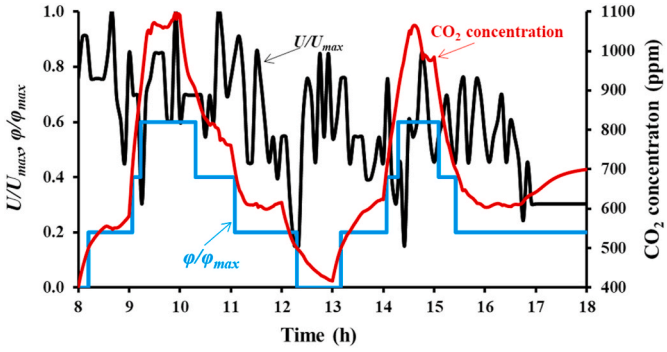

Fig. 8. Dynamic simulation of single-sided demand-controlled natural ventilation using the simplified direct forcing approach. Black lines: dimensionless outdoor wind speeds (U_{max} = 3.3 m s^{-1}); Red lines: indoor CO_2 concentration (ppm) at a monitored location; Blue lines: ratio of window opening angle to the maximum opening angle (50°). (For interpretation of the references to colour in this figure legend, the reader is referred to the Web version of this article.)

boundary and direct forcing approaches, respectively. At the 90° incident angle, the height of the neutral plane decreased from 2.11 m at the upwind side to 1.19 m at the downwind side for the wall boundary method. The height predicted by the direct forcing approach decreased from 2.05 m to 1.55 m. The two methods predicted the same starting point at −0.1 m, but different ending points, 0.3 m and 0.1 m for the wall boundary method and direct forcing approach, respectively. At the 135° incident angle, at the same horizontal location, the wall boundary method predicted two neutral plane heights. However, the direct forcing approach could not reproduce the complicated shape of the neutral plane. At the 180° incident angle, the height of the neutral plane estimated by the wall boundary method depended on the horizontal location; the average value was 1.67 m. The height of the neutral plane predicted by the direct forcing approach was nearly independent of the horizontal locations: 1.75 m.

3.3. Dynamic modeling

The objective of the dynamic modeling was to demonstrate the performance of the direct forcing approach when representing the dynamic window operations that provide better natural ventilation and control over the CO_2 concentration level in a room. The direct forcing approach showed good overall performance, especially when the wind approached at angles between 0° and 135°. The direct forcing approach was applied to a CFD model to study the dynamic CO_2 variations in a

cubical building with single-sided natural ventilation. The external wind speeds were sampled every 5 min from a local weather station on the roof of the building and normalized by the maximum wind speed during the sampled 10 hours. The wind direction was almost constant during those 10 hours. At the start of the dynamic simulation, the windows were closed and an occupant scheduled to enter the room. The CO_2 concentration in the room elevated, due to the presence of the occupant. When the CO_2 level was above 500 ppm, the window was operated to open. The maximum angle of opening was set to 50°. The ratio of the window's opening angle to the maximum opening angle is shown in Fig. 8. Variations in the CO_2 concentration was the combined result of the window operation and number of occupants. According to the rule of demand control (see Table 2), the maximum opening ratio needed to be 60% to maintain the CO_2 level below the set-point value of 1100 ppm. During hours 12 and 13, the window was closed and the natural ventilation rate was zero. Since there were no occupants, the CO_2 concentration at the monitored position began to decrease, due to the diffusion effect. The CO_2 concentration in the room did not reach a steady state within 1 hour. Fig. 8 shows that the direct forcing approach can be implemented to facilitate the dynamic modeling of natural ventilation with pre-defined control algorithms and used to evaluate the daily or weekly performance of those control algorithms.

The maximum dynamic CO_2 concentration was compared to a steady-state CO_2 concentration when four persons were in the test building (see Fig. 2). The steady-state calculation was applied to the maximum wind speed of 3.3 m s^{-1} (see Fig. 8). According to Fig. 5, the ventilation rate was about 0.05 m^3/s. On average, a person breathes out 500 L of CO_2 per day (5.78 $\times$ 10^{-6} m^3 s^{-1}). The increase in total CO_2 concentration in the room could thus be calculated as $4 \times 5.78 \times 10^{-6}/0.05 \times 10^{6}$. The steady-state CO_2 concentration was about 864 ppm. The maximum CO_2 concentration was 1096 ppm, according to the dynamic calculation. One reason for the difference was the constant (3.5 s^{-1}) and higher external wind speeds for the steady-state calculation. The wind speeds for the dynamic calculation varied from 0.5 to 3.3 m s^{-1}. Therefore, CO_2 accumulated in the room during the dynamic operation of the windows. Another reason is the assumption of well-mixing for the steady-state calculation. The CO_2 concentration was assumed to be uniform in the room for the steady-state calculation. However, the CO_2 distribution for the dynamic case was non-uniform due to air circulation (see Fig. 10). Compared to the steady-state situation, more CO_2 stayed in the room in the dynamic situation. The comparison between the maximum CO_2 concentration for the dynamic case and uniform steady-state CO_2 concentration justified the rationale for using the direct forcing approach in the dynamic simulation.

4. Discussion

The direct forcing approach showed good performance for various wind speeds when the wind approached perpendicular to the window aperture. Satisfactory performance was also achieved when the wind's incident angle was smaller than 135°.The direct forcing approach could not reproduce the complicated shape of the neutral plane for wind with an incident angle of 135° (see Fig. 7). At a 180° incident angle, the volume flow rate through the window aperture predicted by the direct forcing approach was about half of that calculated by the wall boundary method. The reason for the deviation could be explored by studying the forces (see Fig. 9) induced by treating the window surface as a wall. The static pressure (P), wall shear stresses (τ), and Reynolds stresses (R) are shown in Fig. 9 for different wind speeds and incident angles. The forces were normalized by the dynamic pressure based on the reference wind speed at the inlet. The wall shear and Reynolds stresses were scaled up by factors of 1000 and 100, respectively. The Reynolds stresses (R_{ij}) were approximated by the Boussinesq relationship:

$$R_{ij} = \mu_t \left(\frac{\partial U_i}{\partial x_j} + \frac{\partial U_j}{\partial x_i} \right) - \frac{2}{3} \rho k \delta_{ij} \tag{4}$$

where μ_t is the turbulent viscosity, k is the turbulent kinetic energy, and δ_{ij} is the Kronecker delta.

When the approaching wind was perpendicular to the window aperture, the normalized static pressure on the window surface increased from 0.75 to 0.93 with the increase in wind speed from 3.5 m s^{-1} to 12 m s^{-1}. The dominant dimensionless Reynolds stresses were in the normal direction and varied between -0.85×10^{-2} and -1.25×10^{-2}. The direct forcing approach using Equations (1) and (2) represented these forces well. Therefore, the direct forcing approach showed good agreement with the wall boundary method under these circumstances. The wall shear stresses were invariant with the increase in wind speed. The dominant normalized wall shear stresses were -0.20×10^{-3} in the horizontal direction and 0.34×10^{-3} in the vertical direction. Neglecting the effect of wall shear stresses in the direct forcing approach did not induce significant errors as compared to the wall boundary method.

At the 45° incident angle, the dimensionless static pressure dropped to 0.45, as compared to at a 0° incident angle. This is why the airflow

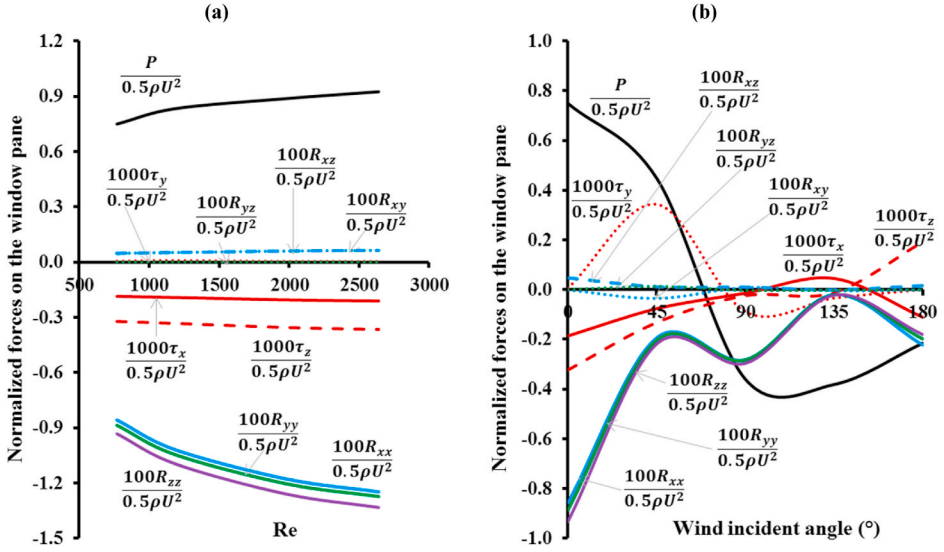

Fig. 9. Static pressure, wall shear stresses, and Reynolds stresses for the window surface open at 30° under different: (a) Reynolds numbers and (b) wind incident angles.

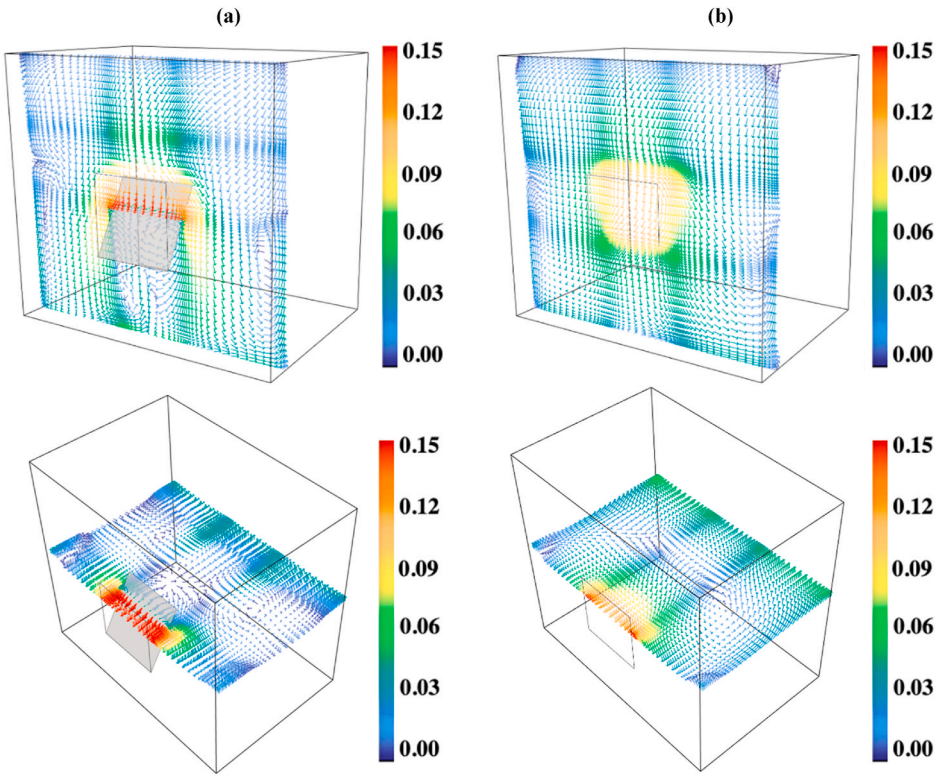

Fig. 10. Comparison of indoor airflow patterns between: (a) the wall boundary method and (b) simplified direct forcing approach.

volume rate predicted by the direct forcing approach at 45° was larger than that at 0°. The dimensionless wall shear stress in the y direction increased to 0.34×10^{-3} and caused the volume flow rate predicted by the wall boundary method to decrease compared to the value at 0°. At the 90° incident angle, neglecting the wall shear stress in the y direction also led to an overestimation of the volume flow rate by the direct forcing approach, as compared to the wall boundary method. The dimensionless wall shear and Reynolds stresses were very small. Hence, the relative deviation in the volume flow rate between the two approaches was also very small. However, the difference in shapes of the neutral plane at the 135° incident angle were large, which may be due to other constraints on the wall boundary method, which are discussed below. The dimensionless static pressure was 0.22 at the 180° incident angle, the smallest among the different wind directions. This is why the volume flow rate predicted by the wall boundary method was the largest at the 180° incident angle. The wall shear and Reynolds stresses became larger than those at 135°. These forces were not well represented in the direct forcing approach for 180° and led to large errors in volume flow rate between the two approaches.

At the 135° incident angle, the substantial difference in the shapes of the neutral plane may be due to the inability of the direct forcing approach to set the normal velocity to zero. Therefore, the airflow patterns obtained by the two approaches were different near the region occupied by the window surface. The airflow patterns near the window surface are demonstrated in Fig. 10. It can be seen that the two approaches predicted similar indoor airflow patterns except near the window surface. The direct forcing approach neglected the constraint of zero normal velocity on the wall surface, inducing errors in airflow patterns near the window surface. Hence, the direct forcing approach was not able to represent the shape of the neutral plane at the 135° incident angle.

Attention also needs to be paid to the volume flow rate through the window aperture. Due to the window surface of the hopper windows, the volume flow rate was generally not the same as the indoor ventilation rate because part of the volume flow rate was directly reflected outside by the hopper window. The indoor ventilation rate must be determined by the tracer gas decay method in CFD. For example, the indoor ventilation rate was 0.027 $m^3\ s^{-1}$ and 0.033 $m^3\ s^{-1}$ for the wall boundary method and direct forcing approach, respectively, when the reference wind speed was 3.5 m s^{-1} and the incident angle 0°. The indoor ventilation rates were much lower than the volume flow rate through the window aperture.

5. Conclusions

Dynamic modeling of natural ventilation can be challenging using conventional CFD simulations that treat windows as wall boundary surfaces. This study presents a direct forcing approach to implement dynamic window operation into CFD simulations. The direct forcing approach marks a band of computational cells according to the window position, and adds an ad-hoc body force to the momentum equations and turbulence production term to the kinetic energy equation. Compared to the wall boundary method, the direct forcing approach showed good performance with regards to predicting the volume flow rate through the window aperture. At high external wind speeds (12 m s^{-1}), the relative deviation between the wall boundary and direct forcing approaches was 2.2%, while such deviation increased to 14% at low external wind speeds (3.5 m s^{-1}). The direct forcing approach was able to accurately calculate the height of the neutral plane when the approaching wind was perpendicular to the aperture of the hopper window. The height of the neutral plane was 1.60 m, irrespective of the external wind speed. When the wind incident angle was smaller than 135°, the direct forcing approach was able to satisfactorily predict the profile of the neutral plane for the window aperture. The direct forcing approach could not reproduce the complicated shape of the neutral plane for a wind incident angle of 135°. The substantial difference might be due to the inability of the direct forcing approach to impose zero normal velocity on the wall surface. At a 180° incident angle, the volume flow rate through the window aperture predicted by the direct forcing approach was about half of that calculated by the wall boundary

method, because the impacts of wall shear and Reynolds stresses became more significant and were not well represented by the direct forcing approach for 180°. The direct forcing approach showed good performance with regards to the dynamic CO_2 variations in a cubical building with single-sided natural ventilation, as well as for evaluating the daily or weekly performances of control algorithms. In the future, the direct forcing approach should consider the influence of the wall shear stresses and zero normal velocity to obtain higher accuracy. Nevertheless, the direct forcing approach is promising for dynamic simulations of natural ventilation and testing window control algorithms in the time range of one day to one week.

The development of the direct forcing approach is instrumental for different natural ventilation control algorithms such as model predictive control. The wall boundary method is very difficult to use for dynamic simulations, and prevents performance tests of control algorithms. For example, a CFD model using the direct forcing approach to represent windows can be applied as a testbed to evaluate whether model predictive control is able to maintain lower indoor CO_2 concentrations as compared to other control algorithms. One limitation of this research is that current models do not consider thermal conditions and real buildings in an urban setting. Future work will incorporate buoyancy force due to temperature gradient, and a model will be developed and tested for a real building.

Declaration of competing interest

The authors declare that they have no known competing financial interests or personal relationships that could have appeared to influence the work reported in this paper.

References

[1] M. Heidarinejad, D.A. Dalgo, N.W. Mattise, J. Srebric, Personalized cooling as an energy efficiency technology for city energy footprint reduction, J. Clean. Prod. 171 (2018) 491–505.

[2] P. Shen, Impacts of climate change on U.S. building energy use by using downscaled hourly future weather data, Energy Build. 134 (2017) 61–70.

[3] X. Cao, X. Dai, J. Liu, Building energy-consumption status worldwide and the state-of-the-art technologies for zero-energy buildings during the past decade, Energy Build. 128 (2016) 198–213.

[4] M. Gil-Baez, Á. Barrios-Padura, M. Molina-Huelva, R. Chacartegui, Natural ventilation systems in 21st-century for near zero energy school buildings, Energy 137 (2017) 1186–1200.

[5] C. Heracleous, A. Michael, Assessment of overheating risk and the impact of natural ventilation in educational buildings of Southern Europe under current and future climatic conditions, Energy 165 (2018) 1228–1239.

[6] H.L Gough, J.F Barlow, Z. Luo, M.-F. King, C.H Halios, C.S.B Grimmond, Evaluating single-sided natural ventilation models against full-scale idealised measurements: impact of wind direction and turbulence, Build. Environ. 170 (2020) 106556.

[7] H.L. Gough, Z. Luo, C.H. Halios, M.F. King, C.J. Noakes, C.S.B. Grimmond, J. F. Barlow, R. Hoxey, A.D. Quinn, Field measurement of natural ventilation rate in an idealised full-scale building located in a staggered urban array: comparison between tracer gas and pressure-based methods, Build. Environ. 137 (2018) 246–256.

[8] Y. Liu, Y. Hu, Y. Xiao, J. Chen, H. Huang, Effects of different types of entrances on natural ventilation in a subway station, Tunn. Undergr. Space Technol. 105 (2020) 103578.

[9] Y. Arinami, S.I. Akabayashi, Y. Tominaga, J. Sakaguchi, Performance evaluation of single-sided natural ventilation for generic building using large-eddy simulations: effect of guide vanes and adjacent obstacles, Build. Environ. 154 (2019) 68–80.

[10] W. Pan, S. Liu, S. Li, X. Cheng, H. Zhang, Z. Long, T. Zhang, Q Chen, A model for calculating single-sided natural ventilation rate in an urban residential apartment, Build. Environ. 147 (2019) 372–381.

[11] T.S. Larsen, C. Plesner, V. Leprince, F.R. Carrié, A.K. Bejder, Calculation methods for single-sided natural ventilation, Energy Build. 177 (15) (2018) 279–289.

[12] M.-F. King, H.L. Gough, C. Halios, J.F. Barlow, A. Robertson, R. Hoxey, C. J. Noakes, Investigating the influence of neighbouring structures on natural ventilation potential of a full-scale cubical building using time-dependent CFD, J. Wind Eng. Ind. Aerod. 169 (2017) 265–279.

[13] S. Marzbana, L. Ding, F. Fiorito, An evolutionary approach to single-sided ventilated façade design, in: International High- Performance Built Environment Conference – A Sustainable Built, 2017.

[14] J. Wang, S. Wang, T. Zhang, F. Battagli, Assessment of single-sided natural ventilation driven by buoyancy forces through variable window configurations, Energy Build. 139 (2017) 762–799.

[15] J. Zhou, C. Ye, Y. Hu, H. Hemida, G. Zhang, W. Yang, Development of a model for single-sided, wind-driven natural ventilation in buildings, Build. Serv. Eng. Technol. 38 (2017) 381–399.

[16] Y. Chen, Z. Tong, W. Wu, H. Samuelson, A. Malkawi, L. Norford, Achieving natural ventilation potential in practice: control schemes and levels of automation, Appl. Energy 235 (2019) 1141–1152.

[17] R. Yao, B. Li, K. Steemers, A. Short, Assessing the natural ventilation cooling potential of office buildings in different climate zones in China, Renew. Energy 34 (12) (2009) 2697–2705.

[18] J. Chen, G.S. Brager, G. Augenbroe, X. Song, Impact of outdoor air quality on the natural ventilation usage of commercial buildings in the US, Appl. Energy 235 (2019) 673–684.

[19] R.G. Southall, An assessment of the potential of supply-side ventilation demand control to regulate natural ventilation flow patterns and reduce domestic space heating consumption, Energy Build. 168 (2018) 201–214.

[20] J. Sykes, Control of Naturally Ventilated Buildings: a Model Predictive Control Approach, The Department of Civil and Structural Engineering, University of Sheffield, 2017, p. 187.

[21] A. Belleri, R. Lollini, S.M. Dutton, Natural ventilation design: an analysis of predicted and measured performance, Build. Environ. 81 (2014) 123–138.

[22] R. Ramponi, I. Gaetani, A. Angelotti, Influence of the urban environment on the effectiveness of natural night-ventilation of an office building, Energy Build. 78 (2014) 25–34.

[23] A. Aflaki, N. Mahyuddin, Z.A. Mahmoud, M.R. Baharum, A review on natural ventilation applications through building façade components and ventilation openings in tropical climates, Energy Build. 101 (2015) 153–162.

[24] W. Wu, J. Zhai, G. Zhang, P.V. Nielsen, Evaluation of methods for determining air exchange rate in a naturally ventilated dairy cattle building with large openings using computational fluid dynamics (CFD), Atmos. Environ. 63 (2012) 179–188.

[25] G. Remion, B. Moujalled, M. El Mankibi, Review of tracer gas-based methods for the characterization of natural ventilation performance: comparative analysis of their accuracy, Build. Environ. 160 (2019) 106180.

[26] W. Wu, G. Zhang, P. Kai, Ammonia and methane emissions from two naturally ventilated dairy cattle buildings and the influence of climatic factors on ammonia emissions, Atmos. Environ. 61 (2012) 232–243.

[27] H.L. Gough, Z. Luo, C.H. Halios, M.F. King, C.J. Noakes, C.S.B. Grimmond, J. F. Barlow, R. Hoxey, A.D. Quinn, Field measurement of natural ventilation rate in an idealised full-scale building located in a staggered urban array: comparison between tracer gas and pressure-based methods, Build. Environ. 137 (2018) 246–256.

[28] A. O' Donovan, P.D. O' Sullivan, M.D. Murphy, Predicting air temperatures in a naturally ventilated nearly zero energy building: calibration, validation, analysis and approaches, Appl. Energy 250 (2019) 991–1010.

[29] I. Oropeza-Perez, P.A. Østergaard, Potential of natural ventilation in temperate countries – a case study of Denmark, Appl. Energy 114 (2014) 520–530.

[30] Y. Liu, Y. Xiao, J. Chen, G. Augenbroe, T. Zhou, A network model for natural ventilation simulation in deep buried underground structures, Build. Environ. 153 (2019) 288–301.

[31] T. Schulze, U. Eicker, Controlled natural ventilation for energy efficient buildings, Energy Build. 56 (2013) 221–232.

[32] H. Wang, P. Karava, Q. Chen, Development of simple semiempirical models for calculating airflow through hopper, awning, and casement windows for single-sided natural ventilation, Energy Build. 96 (2015) 373–384.

[33] H. Wang, Q. Chen, A new empirical model for predicting single-sided, wind-driven natural ventilation in buildings, Energy Build. 54 (2012) 386–394.

[34] P. Stamatopoulos, P. Drosatos, N. Nikolopoulos, D. Rakopoulos, Determination of a methodology to derive correlations between window opening mass flow rate and wind conditions based on CFD results, Energies 12 (9) (2019).

[35] K. Kosutova, T. van Hooff, C. Vanderwel, B. Blocken, J. Hensen, Cross-ventilation in a generic isolated building equipped with louvers: wind-tunnel experiments and CFD simulations, Build. Environ. 154 (2019) 263–280.

[36] H. Shetabivash, Investigation of opening position and shape on the natural cross ventilation, Energy Build. 93 (2015) 1–15.

[37] M.Z.I. Bangalee, S.Y. Lin, J.J. Miau, Wind driven natural ventilation through multiple windows of a building: a computational approach, Energy Build. 45 (2012) 317–325.

[38] F. Muhsin, W.F.M. Yusoff, M.F. Mohamed, A.R. Sapian, CFD modeling of natural ventilation in a void connected to the living units of multi-storey housing for thermal comfort, Energy Build. 144 (2017) 1–16.

[39] Y. Jiang, D. Alexander, H. Jenkins, R. Arthur, Q. Chen, Natural ventilation in buildings: measurement in a wind tunnel and numerical simulation with large-eddy simulation, J. Wind Eng. Ind. Aerod. 91 (3) (2003) 331–353.

[40] Y. Arinami, S.I. Akabayashi, Y. Tominaga, J. Sakaguchi, Performance evaluation of single-sided natural ventilation for generic building using large-eddy simulations: effect of guide vanes and adjacent obstacles, Build. Environ. 154 (2019) 68–80.

[41] C.R. Chu, B.F. Chiang, Wind-driven cross ventilation in long buildings, Build. Environ. 80 (2014) 150–158.

[42] C.R. Chu, Y.H. Chiu, Y.-T. Tsai, S.L. Wu, Wind-driven natural ventilation for buildings with two openings on the same external wall, Energy Build. 108 (2015) 365–372.

[43] S. Liu, W. Pan, Q. Cao, Z. Long, Y. Jiang, Q. Chen, CFD simulations of natural cross ventilation through an apartment with modified hourly wind information from a meteorological station, Energy Build. 195 (2019) 16–25.

[44] Y. Tao, K. Inthavong, J. Tu, A numerical investigation of wind environment around a walking human body, J. Wind Eng. Ind. Aerod. 168 (2017) 9–19.

[45] W. Wu, B. Wang, A. Malkawi, N. Yoon, Z. Sehovic, B. Yan, A method toward real-time CFD modeling for natural ventilation, Fluid 3 (4) (2018) 101.
[46] A. Ltd, Fluent Help Release 17.0, Ansys Inc., Canonsburg, PA, USA, 2017.
[47] Y. Tominaga, A. Mochida, R. Yoshie, H. Kataoka, T. Nozu, M. Yoshikawa, T. Shirasawa, AIJ guidelines for practical applications of CFD to pedestrian wind environment around buildings, J. Wind Eng. Ind. Aerod. 96 (10) (2008) 1749–1761.
[48] P.J. Richards, S.E. Norris, Appropriate boundary conditions for computational wind engineering models revisited, J. Wind Eng. Ind. Aerod. 99 (4) (2011) 257–266.
[49] T.H. Shih, W.W. Liou, A. Shabbir, Z. Yang, J. Zhu, A new k-ε eddy viscosity model for high Reynolds number turbulent flows, Comput. Fluids 24 (3) (1995) 227–238.